LETTER

An optical–frequency synthesizer using integrated photonics

Daryl T. Spencer[1]*, Tara Drake[1], Travis C. Briles[1,2], Jordan Stone[1], Laura C. Sinclair[1], Connor Fredrick[1,2], Qing Li[3], Daron Westly[3], B. Robert Ilic[3], Aaron Bluestone[4], Nicolas Volet[4], Tin Komljenovic[4], Lin Chang[4], Seung Hoon Lee[5], Dong Yoon Oh[5], Myoung-Gyun Suh[5], Ki Youl Yang[5], Martin H. P. Pfeiffer[6], Tobias J. Kippenberg[6], Erik Norberg[7], Luke Theogarajan[4], Kerry Vahala[5], Nathan R. Newbury[1], Kartik Srinivasan[3], John E. Bowers[4], Scott A. Diddams[1,2] & Scott B. Papp[1,2]*

Optical-frequency synthesizers, which generate frequency-stable light from a single microwave-frequency reference, are revolutionizing ultrafast science and metrology, but their size, power requirement and cost need to be reduced if they are to be more widely used. Integrated-photonics microchips can be used in high-coherence applications, such as data transmission[1], highly optimized physical sensors[2] and harnessing quantum states[3], to lower cost and increase efficiency and portability. Here we describe a method for synthesizing the absolute frequency of a lightwave signal, using integrated photonics to create a phase-coherent microwave-to-optical link. We use a heterogeneously integrated III−V/silicon tunable laser, which is guided by nonlinear frequency combs fabricated on separate silicon chips and pumped by off-chip lasers. The laser frequency output of our optical-frequency synthesizer can be programmed by a microwave clock across 4 terahertz near 1,550 nanometres (the telecommunications C-band) with 1 hertz resolution. Our measurements verify that the output of the synthesizer is exceptionally stable across this region (synthesis error of 7.7×10^{-15} or below). Any application of an optical-frequency source could benefit from the high-precision optical synthesis presented here. Leveraging high-volume semiconductor processing built around advanced materials could allow such low-cost, low-power and compact integrated-photonics devices to be widely used.

The electronics revolution that began in the mid-twentieth century was driven in part by advances related to the synthesis of radio and microwave-frequency signals for applications in radar, navigation and communications systems. This formed a foundation for more recent technologies of wide impact, such as the Global Positioning System and cellular communications. Direct-digital synthesis now operates at >10 GHz rates with watt-scale power. Despite the ubiquity of electronic synthesis, no comparable technology existed for electromagnetic signals in the optical domain until the introduction of the self-referenced optical-frequency comb[4,5]. An optical-frequency comb can provide the critical phase-coherent link between microwave and optical domains, with an output consisting of an array of optical modes having frequencies given exactly by $\nu_n = n f_{rep} + f_{ceo}$, where f_{rep} and f_{ceo} are microwave frequencies and n is an integer. Over the past two decades, optical-frequency synthesizers using mode-locked-laser frequency combs have been demonstrated[6,7]. The optical-synthesizer output, derived from a reference clock, is invaluable for coherent light detection and ranging[7], atomic and molecular spectroscopy and optical communications. Optical-frequency-comb technology has also matured so that a typical erbium-fibre comb system requires approximately 2 W of optical pump power[8].

A new opportunity for chip-integrated optical-frequency synthesis has emerged with development in heterogeneously integrated photonics[9] and photonic-chip microresonator frequency combs, or microcombs[10–17]. Microresonators pumped by a continuous-wave

(CW) laser generate a parametric four-wave mixing comb in dielectric media. Relying on waveguide confinement and high nonlinearity of the integrated photonics, microresonators provide a route to comb generation with only milliwatts of input power[17] and high pump-conversion efficiency[18]. Precise waveguide group-velocity dispersion (GVD) control[19], combined with the realization of low-noise dissipative Kerr solitons (DKSs)[20–22], has led to octave-spanning optical spectra with dispersive waves[23–25] to enhance the signal-to-noise ratio in microcomb carrier-envelope-offset frequency (f_{ceo}) detection[26–28]. In parallel, through heterogeneous integration it has become possible to seamlessly combine active and passive components, such as semiconductor lasers and amplifiers, electro-optic modulators, passive waveguides, photodiodes and complementary metal–oxide–semiconductor (CMOS) electronics on a silicon-chip platform[9], and specifically to implement phase-locking of integrated lasers to microcombs[29,30]. Our work makes use of Kerr-soliton frequency combs and silicon photonics to realize optical-frequency synthesis derived phase-coherently from an electronic clock.

Mirroring the framework of most traditional optical and microwave synthesizers, our system is composed of a tunable laser oscillator that we phase-lock to a stabilized microcomb reference. Figure 1a presents the concept of a future integrated synthesizer, and Fig. 1b indicates the connections between the integrated tunable laser and the chip-based Kerr-comb components that are used in this work. We use the C-band tunability, narrow linewidth and rapid frequency control of a III−V/silicon ring-resonator[9] laser as the synthesizer output, and the phase-coherent microwave-to-optical connection of a fully stabilized DKS frequency comb. The DKS dual comb consists of an octave-bandwidth, silicon nitride comb with 1 THz mode spacing and a C-band-spanning, fused-silica comb with 22 GHz mode spacing. By phase-stabilizing both comb spacings ($f_{rep,THz}$ and $f_{rep,GHz}$) and the silicon nitride comb's offset frequency, $f_{ceo,THz}$, we establish the precise factor of 19,403,904 phase-coherent multiplication from 10 MHz to the optical domain. With this tunable-laser and frequency-comb system, we demonstrate synthesis across a 4-THz segment of the C-band by programming and dynamically stepping the output frequency; see Fig. 1c–e. As the role of any synthesizer is to output a phase-coherently multiplied version of the input clock, we characterize the optical synthesizer primarily through its fluctuations with an out-of-loop frequency comb derived from the same clock. A fully integrated synthesizer, realized by using, improving and connecting the chip components that we describe, would be a powerful tool for many applications (see Methods).

To demonstrate the optical-frequency synthesizer, we carry out a series of experiments characterizing its output frequency. Standard spectrometer or interferometer measurements readily verify system performance at the megahertz (or 10^{-8}) level. By measuring the synthesizer with an auxiliary self-referenced erbium-fibre comb, we constrain the frequency error between the output and the synthesizer's
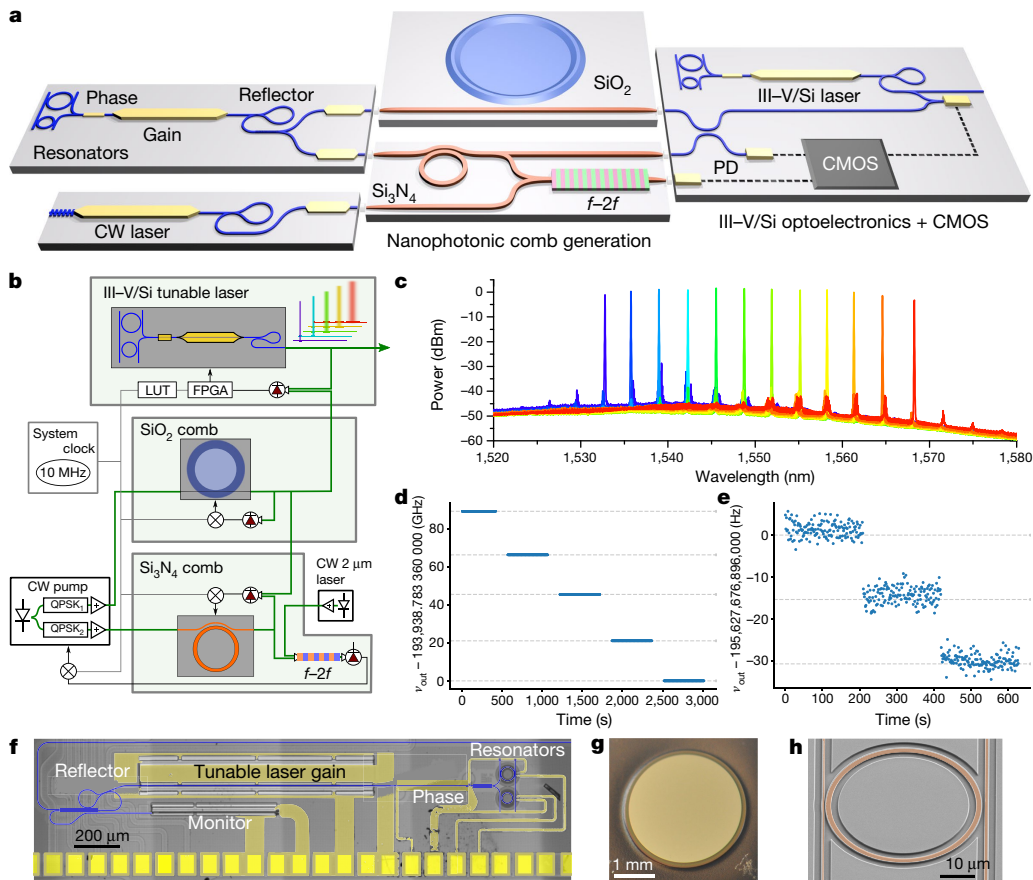
Fig. 1 | Accurate optical synthesis with an integrated laser and DKS dual-comb system. a, Conceptual integrated optical-frequency synthesizer with digital control and f–$2f$ stabilization, using the microcombs and tunable laser of this work. PD, photodetector. **b,** Our optical synthesizer is composed of an integrated tunable laser and chip-based Kerr-comb generators. Green boxes indicate the tabletop subsystems including the chips, and how they connect. The CW pumping laser for some experiments is a second integrated laser; see Methods. The tunable laser is synthesized by phase-locking to the stabilized combs, using a look-up table (LUT) and FPGA. QPSK, quadrature phase shift key modulator. **c,** Optical spectra of the laser across 32 nm. **d, e,** Measurements of the synthesizer output as it is stepped. The data indicate the deviation between the synthesizer output ν_{out} and its setpoint for mode-hopping across the 22-GHz SiO$_2$ modes (**d**) and for application of precise frequency steps of 15.36 Hz (**e**). **f,** Scanning electron microscope (SEM) image of the heterogeneous III−V/Si tunable laser with false colour electrodes (yellow) and waveguides (blue). **g,** Photograph of the SiO$_2$-based wedge microresonator. **h,** SEM image of the Si$_3$N$_4$ THz resonator with false colour imposed on the waveguide regions.

setpoint to <1.5 Hz. Beyond demonstration of the integrated-photonics architecture, the core result of our work is verification that the synthesizer offers sufficient phase control and synchronization in microwave-to-optical conversion (as do the auxiliary comb and our frequency-counting electronics) to reveal a stable phase correlation between the CW output and the radiofrequency (RF) clock. Hence, the statistical fluctuations that lead to the synthesizer's instability, and our measurement of these, offer the complete description of the synthesizer's frequency performance.

The chip-based integrated components of the synthesizer—the tunable laser (Fig. 1f) and DKS frequency combs (Fig. 1g and h)—and their key connections with non-integrated components are emphasized in Fig. 1b. An external cavity pump laser is used to generate both of the DKS combs, using independent control with single-sideband frequency shifters and erbium amplification for each comb. An octave-spanning single-pulse soliton is generated in a Si$_3$N$_4$ planar waveguide-coupled resonator. In addition to the anomalous GVD profile, waveguide-dispersion engineering creates dispersive-wave peaks in optical power that appear at 999 nm and 2,190 nm, owing to the zero-integrated GVD starting from the pump wavelength. With a radius of 23 μm, the threshold for octave-spanning spectra is brought to below 50 mW of on-chip pump power[24], at the expense of a $f_{rep,THz}$ of 1.014 THz that cannot be easily photodetected and reduced to a microwave frequency with conventional electronics. Rather, we rely on a second frequency comb to bridge the gap between Si$_3$N$_4$ THz comb modes.

To do this, an SiO$_2$ wedge-based whispering-gallery-mode resonator with a quality factor (Q) of 180 million is used to create a DKS frequency comb at $f_{rep,GHz} \approx 22$ GHz (ref. [22]). As the threshold for soliton-comb generation scales inversely to both the repetition rate and Q^2, use of an SiO$_2$ device is important for low-power operation. The repetition frequency of 22 GHz is photodetected and phase-locked to the RF clock. This first step in the microwave-to-optical frequency chain (Fig. 2a) from $f_{clk} = 10$ MHz to 22 GHz partially stabilizes the SiO$_2$ reference comb to guide tunable laser synthesis; see Fig. 2b. The second step is detection of the 1.014 THz frequency spacing between Si$_3$N$_4$ comb teeth, which we accomplish using the 46th relative comb line from the SiO$_2$ comb. Operationally, we measure $f_{rep,THz}$ by detecting the optical heterodyne beat note between the two combs 1 THz away from the pump. We phase-lock this signal to a synthesized radiofrequency, $f_1 = \alpha f_{clk}$ (where α is the ratio of two integers), after removing the relative contributions from the single-sideband frequency shifters and feeding back to the frequency of the Si$_3$N$_4$ pump laser[31,32]. Thus, we stabilize $f_{rep,THz}$ and transfer the f_{clk} stability to 1.014 THz. The frequency of each of the Si$_3$N$_4$ THz comb lines with negative offset frequency and mode number $N = 192$ is then given by:

$$\nu_{THz} = N f_{rep,THz} - f_{ceo,THz}$$
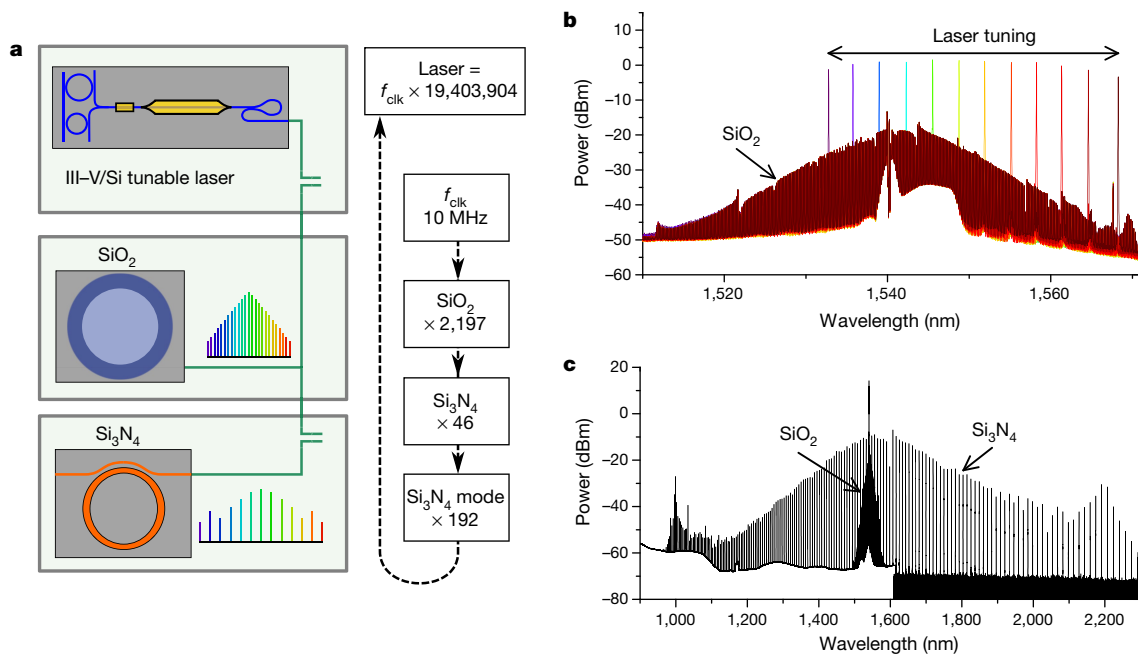$$\nu_{THz,pump} = 192(46 f_{rep,GHz} + \alpha f_{clk}) - f_{ceo,THz} \quad (1)$$

Fig. 2 | Optical spectra of the integrated devices. a, Schematic diagram of spectral combination with the integrated devices, and the frequency chain used to multiply the 10-MHz clock to the optical domain. **b**, Combined spectrum of the SiO_2 22-GHz wedge microcomb and the heterogeneously integrated III−V/Si tunable laser in the telecommunication C-band. **c**, Combined spectrum of the octave-spanning Si_3N_4 THz microcomb and the 22-GHz SiO_2 wedge microcomb, as measured on two optical spectrum analysers.

Next, $f_{ceo,THz}$ locking is achieved by using the octave-spanning relationship of the THz lines at 1,998 nm and dispersive wave peak at 999 nm (Fig. 2c). To aid f–$2f$ self-referencing (which enables determination of the absolute frequency of each comb line), an independent diode laser and thulium-doped fibre amplifier at 1,998 nm supply 9 mW to a waveguide periodically poled lithium niobate (PPLN) device to achieve 34 dB signal-to-noise ratio (SNR) on $f_{ceo,THz}$. Similar monolithic second-harmonic generation and amplifier technologies have been demonstrated and could be integrated with our system (see Methods). After detecting two heterodyne beats with the THz comb, f_{999} and f_{1998}, each beat note is digitally divided by 64 and 32, respectively, and frequency mixing yields an $f_{ceo,THz}$ signal, $f_{ceo,THz}/64 = f_{999}/64 - f_{1998}/32$.
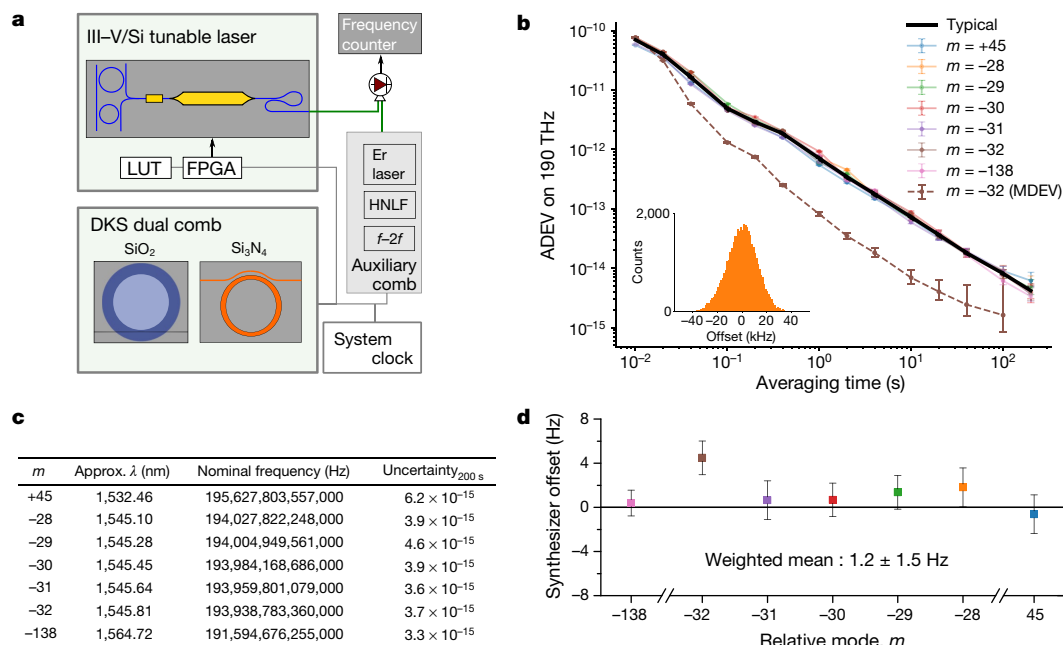

Fig. 3 | Stable optical synthesis with out-of-loop verification. a, Tunable laser locking, and frequency counting with the auxiliary comb. HNLF, highly nonlinear fibre. **b**, Measured overlapping Allan deviation (ADEV) and modified Allan deviation (MDEV) of the frequency synthesizer. In comparing 10-ms counter-gate time acquisitions, the $1/\tau$ slope is consistent with a stable, phase-locked synthesizer, and the histograms of 500 s of data (inset for relative mode $m = -28$ only) show a Gaussian profile. Error bars indicating 95% confidence intervals are derived using flicker noise estimates (see Methods). **c**, Table of nominal frequencies and uncertainty at 200 s as the synthesizer is stepped across the C-band. **d**, Overview of the accuracy and precision of the synthesizer frequency. The ADEV at 100 s is used to estimate the uncertainty of each synthesizer output, and the weighted mean of the seven data points is reported with a 95% (t distribution) confidence interval.

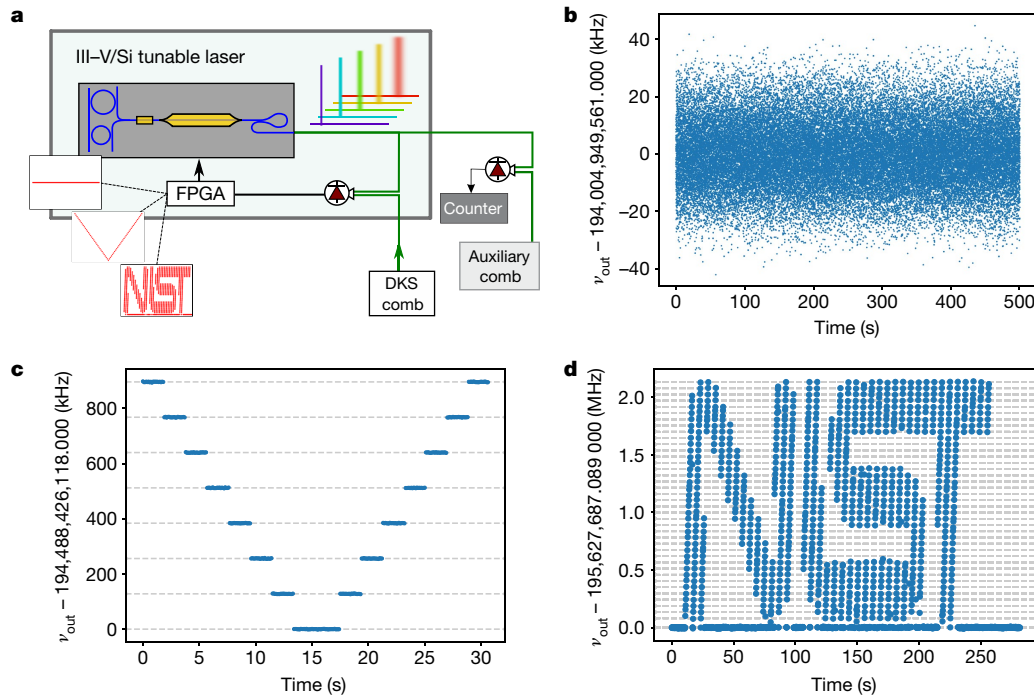| m	Approx. λ (nm)	Nominal frequency (Hz)	Uncertainty$_{200\,s}$
+45	1,532.46	195,627,803,557,000	6.2×10^{-15}
−28	1,545.10	194,027,822,248,000	3.9×10^{-15}
−29	1,545.28	194,004,949,561,000	4.6×10^{-15}
−30	1,545.45	193,984,168,686,000	3.9×10^{-15}
−31	1,545.64	193,959,801,079,000	3.6×10^{-15}
−32	1,545.81	193,938,783,360,000	3.7×10^{-15}
−138	1,564.72	191,594,676,255,000	3.3×10^{-15}

Fig. 4 | Arbitrary control of the optical-frequency synthesizer. a, Stepwise control of the tunable-laser offset phase-lock to the DKS comb and frequency counting. **b**, Deviation between the synthesizer output ν_{out} and constant setpoint for 500 s at a 10-ms gate time. **c**, Bidirectional linear ramp of the synthesizer via step control of the laser offset PLL setpoint (100-ms gate). **d**, Arbitrary frequency control of the synthesizer across 40 frequency setpoints to write "NIST". A 30-ms gate time is used to oversample each frequency setpoint by 5 (150-ms pause per point), and every fifth data point is displayed.

Phase-locking this signal to a radiofrequency $f_2 = \beta f_{clk}$, through feedback to the Si_3N_4 pump power, completes the transfer of stability from f_{clk} to all the THz comb lines spanning 130 THz to 300 THz.

The dual-stabilized combs serve as the backbone to guide the heterogeneously integrated III−V/Si tunable laser for arbitrary optical-frequency synthesis across the C-band. The tunable laser consists of InGaAsP multiple-quantum-well epitaxial material that is wafer-bonded onto a lithographically patterned silicon-on-insulator wafer[9]. Bias heaters integrated on the laser's Si-based resonant reflectors and phase section are used to shift the lasing wavelength for initial alignment to the comb lines. By using Si waveguides that have low loss relative to standard telecommunication-grade InP waveguide technology, reduced linewidths of about 300 kHz are achieved. The combined optical spectrum of the SiO_2 comb and integrated laser's tuning range is shown in Fig. 2b. Heterodyning with the DKS dual-comb signal at a relative mode m from the pump creates a signal, f_{beat}^{laser}, for input to a field-programmable gate array (FPGA)-based phased-locked-loop (PLL, Fig. 3a) with a local oscillator of $f_3 = \gamma f_{clk}$, and digital division of 512. This final laser lock to the DKS dual comb produces a fully stabilized, tunable synthesizer output,

$$\nu_{out} = \nu_{THz,pump} + m f_{rep,GHz} + f_{beat}^{laser}$$
$$= f_{clk} \left[192(46 \times 2{,}197 + \alpha) + 2{,}197m - 64\beta + 512\gamma \right] \quad (2)$$

This expression shows that the output of our integrated-photonics synthesizer is uniquely and precisely defined relative to the input clock frequency in terms of user-chosen integers and ratios of integers (α, β, γ).

Agile tuning across SiO_2 comb lines (varying m) and hertz-level tuning resolution on the same comb line (varying γ) have already been presented in Fig. 2b and Fig. 1c, demonstrating synthesizer operation. To explore our synthesizer's phase coherence, we perform an out-of-loop optical-frequency characterization by heterodyning ν_{out} against an auxiliary erbium-fibre laser frequency comb that is fully stabilized to the same f_{clk}. Figure 3 shows results from a study of the tunability and

phase-locked operation of the synthesizer across all comb frequencies by locking to five adjacent SiO_2 comb lines, and to the highest and lowest wavelengths of the laser tuning range. Overlapping Allan deviation (ADEV) analysis of the counted beat notes against the auxiliary comb show the instability improving as $<10^{-12}/\tau$ for all recorded averaging times τ, and reaching an average instability of $(4.2 \pm 0.4) \times 10^{-15}$ at 200 s (Fig. 3b, c). More sophisticated triangular averaging analysis using the modified Allan deviation (MDEV) yields an order of magnitude better instability of $(9.2 \pm 1.4) \times 10^{-14}$ at 1 s. Still, the $1/\tau$ dependence of the ADEV data, which characterizes the fluctuations of the optical-frequency synthesizer, indicates the stable phase relationship between the RF clock and the synthesized optical frequencies. Moreover, the synthesizer performance is consistent with the hydrogen-maser RF clock used in the experiments, indicating that our phase locks of the tunable laser, the Kerr combs and the auxiliary erbium-fibre comb contribute negligible noise. This is the most fundamental metric of an optical synthesizer. From the mean values of the measured beats with the auxiliary comb, we can further analyse potential deviations of the synthesizer output from equation (2). Data compiled from the seven experiments are shown in Fig. 3d with 100-s ADEV error bars plotted, and the weighted mean of all data sets with a 95% confidence interval is (1.2 ± 1.5) Hz. Thus, based on these initial data, we conclude that our integrated-photonics optical synthesizer accurately reproduces the input clock reference within an uncertainty of 7.7×10^{-15}, competitive with commercial optical synthesizers (5×10^{-13} instability at 1 s and accurate to 10^{-14} at 120 s).

To demonstrate the tunability of the optical-frequency synthesizer, we perform two different types of tuning while the laser is locked to the stabilized comb system (Fig. 4). As a baseline, without changing the setpoint of the tunable laser phase-lock, the raw data of the counted auxiliary comb beat note are shown in Fig. 4b after subtraction of the nominally expected frequency for 500 s. We then apply a bidirectional linear ramp over eight levels with a 2-s pause at each level to ensure successful locking (Fig. 4c). Finally, we programme a series of setpoint frequencies to the FPGA PLL box to write out the National Institute of Standards and Technology (NIST) logo (Fig. 4d). Excellent agreement

is found between the expected offset frequencies and the counted beat-note frequencies for all cases, illustrating good dynamic control of the synthesizer.

In summary, the experiments that we present, performed with an optical-frequency synthesizer constructed from integrated photonics, demonstrate that this technology has achieved the high precision and accuracy that formerly has been confined to tabletop mode-locked laser frequency-comb devices. For further integration of the laser and Kerr combs used in our experiments, targeted improvements should be made to increase microresonator Q for lower-power operation, to improve the intensity of the Si_3N_4 comb dispersive waves for f–$2f$ stabilization, and to improve the efficiency of second-harmonic generation, guided by the applications that are envisaged for the device.

Online content

1. Rumley, S. et al. Silicon photonics for exascale systems. *J. Lightwave Technol.* **33**, 547–562 (2015).
2. Purdy, T. P., Grutter, K. E., Srinivasan, K. & Taylor, J. M. Quantum correlations from a room-temperature optomechanical cavity. *Science* **356**, 1265–1268 (2017).
3. O'Brien, J. L., Furusawa, A. & Vučković, J. Photonic quantum technologies. *Nat. Photonics* **3**, 687–695 (2009).
4. Hall, J. L. Nobel Lecture: Defining and measuring optical frequencies. *Rev. Mod. Phys.* **78**, 1279–1295 (2006).
5. Hänsch, T. W. Nobel Lecture: Passion for precision. *Rev. Mod. Phys.* **78**, 1297–1309 (2006).
6. Jost, J. D., Hall, J. L. & Ye, J. Continuously tunable, precise, single frequency optical signal generator. *Opt. Express* **10**, 515–520 (2002).
7. Giorgetta, F. R., Coddington, I., Baumann, E., Swann, W. C. & Newbury, N. R. Fast high-resolution spectroscopy of dynamic continuous-wave laser sources. *Nat. Photonics* **4**, 853–857 (2010).
8. Sinclair, L. C. et al. Operation of an optically coherent frequency comb outside the metrology lab. *Opt. Express* **22**, 6996–7006 (2014).
9. Komljenovic, T. et al. Heterogeneous silicon photonic integrated circuits. *J. Lightwave Technol.* **34**, 20–35 (2016).
10. Del'Haye, P. et al. Optical frequency comb generation from a monolithic microresonator. *Nature* **450**, 1214–1217 (2007).
11. Savchenkov, A. A. et al. Tunable optical frequency comb with a crystalline whispering gallery mode resonator. *Phys. Rev. Lett.* **101**, 093902 (2008).
12. Kippenberg, T. J., Holzwarth, R. & Diddams, S. A. Microresonator-based optical frequency combs. *Science* **332**, 555–559 (2011).
13. Moss, D. J., Morandotti, R., Gaeta, A. L. & Lipson, M. New CMOS-compatible platforms based on silicon nitride and Hydex for nonlinear optics. *Nat. Photonics* **7**, 597–607 (2013).
14. Grudinin, I. S., Yu, N. & Maleki, L. Generation of optical frequency combs with a CaF_2 resonator. *Opt. Lett.* **34**, 878–880 (2009).
15. Ferdous, F. et al. Spectral line-by-line pulse shaping of on-chip microresonator frequency combs. *Nat. Photonics* **5**, 770–776 (2011).
16. Papp, S. B. & Diddams, S. A. Spectral and temporal characterization of a fused-quartz-microresonator optical frequency comb. *Phys. Rev. A* **84**, 053833 (2011).
17. Li, J., Lee, H., Chen, T. & Vahala, K. J. Low-pump-power, low-phase-noise, and microwave to millimeter-wave repetition rate operation in microcombs. *Phys. Rev. Lett.* **109**, 233901 (2012).
18. Cole, D. C., Lamb, E. S., Del'Haye, P., Diddams, S. A. & Papp, S. B. Soliton crystals in Kerr resonators. *Nat. Photonics* **11**, 671–676 (2017).
19. Okawachi, Y. et al. Bandwidth shaping of microresonator-based frequency combs via dispersion engineering. *Opt. Lett.* **39**, 3535–3538 (2014).
20. Herr, T. et al. Temporal solitons in optical microresonators. *Nat. Photonics* **8**, 145–152 (2014).
21. Leo, F. et al. Temporal cavity solitons in one-dimensional Kerr media as bits in an all-optical buffer. *Nat. Photonics* **4**, 471–476 (2010).
22. Yi, X., Yang, Q.-F., Yang, K. Y., Suh, M.-G. & Vahala, K. Soliton frequency comb at microwave rates in a high-Q silica microresonator. *Optica* **2**, 1078–1085 (2015).
23. Brasch, V. et al. Photonic chip-based optical frequency comb using soliton Cherenkov radiation. *Science* **351**, 357–360 (2016).
24. Li, Q. et al. Stably accessing octave-spanning microresonator frequency combs in the soliton regime. *Optica* **4**, 193–203 (2017).
25. Pfeiffer, M. H. P. et al. Octave-spanning dissipative Kerr soliton frequency combs in Si_3N_4 microresonators. *Optica* **4**, 684–691 (2017).
26. Jost, J. D. et al. Counting the cycles of light using a self-referenced optical microresonator. *Optica* **2**, 706–711 (2015).
27. Del'Haye, P. et al. Phase-coherent microwave-to-optical link with a self-referenced microcomb. *Nat. Photonics* **10**, 516–520 (2016).
28. Brasch, V., Lucas, E., Jost, J. D., Geiselmann, M. & Kippenberg, T. J. Self-referenced photonic chip soliton Kerr frequency comb. *Light Sci. Appl.* **6**, e16202 (2017).
29. Arafin, S. et al. Power-efficient Kerr frequency comb based tunable optical source. *IEEE Photonics J.* **9**, 6600814 (2017).
30. Arafin, S. et al. Towards chip-scale optical frequency synthesis based on optical heterodyne phase-locked loop. *Opt. Express* **25**, 681–695 (2017).
31. Del'Haye, P., Arcizet, O., Schliesser, A., Holzwarth, R. & Kippenberg, T. J. Full stabilization of a microresonator-based optical frequency comb. *Phys. Rev. Lett.* **101**, 053903–053904 (2008).
32. Papp, S. B. et al. Microresonator frequency comb optical clock. *Optica* **1**, 10–14 (2014).

Author Contributions D.T.S., T.D., T.C.B. and J.S. contributed equally to performing the system measurements and analysing the experimental results. D.T.S., S.A.D. and S.B.P. prepared the manuscript. The integrated devices were fabricated and tested by Q.L., D.W., B.R.I. and K.S. (Si_3N_4); A.B., N.V., T.K., L.C. and E. N. (III–V/Si); and S.H.L., D.Y.O., M.S., K.Y.Y. and K.V. (SiO_2). N.V., L.C.S., C.F., M.H.P.F. and A.B. provided measurement support. T.J.K, E.N., K.V., K.S., N.R.N., L.T., J.E.B., S.A.D. and S.B.P. supervised and led the scientific collaboration. This work is an official contribution of the NIST; not subject to copyright in the United States. The use of trade names is not intended to imply recommendation or endorsement by NIST, nor is it intended to imply that the materials or equipment identified are necessarily the best available for the purpose.

Competing interests The authors declare no competing financial interests.

METHODS

Device and experimental details. The heterogeneously integrated III−V/Si device includes a tunable laser and a semiconductor optical amplifier (SOA). At room temperature, the laser emits up to 4 mW CW power, and the SOA provides an on-chip small-signal gain >10 dB. The laser contains a gain section, a phase section and two microresonators designed for high quality factor. The gain section and the SOA consist of electrically pumped InP-based quantum wells heterogeneously integrated on a Si waveguide[9]. Thermal heating of the Si microresonators and passive phase section is performed with current injection to metal heaters above the waveguides. By intentionally mismatching the radii of the microresonators to make use of the Vernier effect, we can use a narrowband intracavity optical filter to select the desired longitudinal mode for lasing with high side-mode suppression ratio[33]. Precise wavelength tuning and linewidth narrowing is performed by heating the phase section (Extended Data Fig. 1). Phase-locking of the laser to the microcomb is performed by electronically dividing the beat note by 512 and using FPGA-based digital PLL + PI²D feedback (that is, a proportional–integral–derivative controller with two-stage integration) to the gain section of the laser[8]. Other works have also demonstrated high-bandwidth optical-PLL phase locks to frequency combs[29,30]. In the current system, the tunable laser can lock to either the SiO₂ or Si₃N₄ comb lines, which we have shown for $m = -138$, or 3 THz red of the pump laser. The DC linear tuning coefficient of the tunable laser is approximately 200 MHz mA^{-1}.

A commercial external cavity diode laser is used as the shared pump for both microresonator comb generators in all the synthesizer experiments. The output of a 3-dB splitter goes to separate LiNbO₃ single-sideband modulators and erbium-doped fibre amplifiers for each device. Frequency detuning from each microcomb resonance for soliton generation is controlled with an amplified voltage-controlled oscillator and arbitrary waveform generator that produces a voltage ramp. Although complex soliton crystals[18] can form in these devices, single solitons are generated through linear voltage ramps of 5 GHz in 100 ns and 100 MHz in 3 μs, for the Si₃N₄ and SiO₂ microcombs, respectively[34]. Once initiated, feedback to each voltage-controlled oscillator controls $f_{rep,GHz}$ and $f_{rep,THz}$ for the appropriate device. Intensity modulation on the Si₃N₄ microcomb to control $f_{ceo,THz}$ is performed with a free-space acousto-optic modulator, although on-chip SOAs are expected to be viable as well. Lensed fibres with a 2.5-μm spot size are used to couple light on and off the Si₃N₄ chip with 7 dB of insertion loss per facet. During operation, the on-chip pump power for the Si₃N₄ microcomb is about 160 mW, or ten times the threshold for soliton generation. Tapered single-mode fibre is used to couple 80 mW to the SiO₂ microcomb for soliton generation at 12 times the soliton threshold. Recent results show that this platform can be integrated with Si₃N₄ bus waveguides[35]. An offset Pound–Drever–Hall lock is required after ramping to keep the SiO₂ pump frequency at 22 MHz red detuned from resonance[36].

During operation of the optical-frequency synthesizer, the separate single-sideband modulators for each microcomb device create a detectable offset in pump frequencies, about 5 GHz in our experiment. This is readily subtracted from or added to the necessary heterodyne beat notes in the system using an electronic frequency mixer, specifically after $f_{rep,THz}$ detection between comb lines and after the III−V/Si laser heterodyne with the DKS comb. The calibrated gain sign of the tunable-laser feedback loop ensures that the tunable laser is on the appropriate side of the SiO₂ comb modes when electronically subtracting or adding this offset, and knowledge of the absolute difference in pump frequencies is not required for accurate optical-frequency synthesis. We observe non-zero synthesis error when the SNR of any heterodyne beat falls well below the optimal level of 30 dB, but measurements reported here were acquired with sufficient SNR. We also observe and minimize contributions from out-of-loop optical and electrical path lengths, alignment drift, and glitches during long acquisitions. The RF synthesis and phase-locking electronics used in the experiments are benchtop scale, but in the future would make use of CMOS integration[37].

Auxiliary comb details and frequency counting. The auxiliary comb used for out-of-loop verification of the optical-frequency synthesizer consists of a 250-MHz erbium-fibre mode-locked laser frequency comb[38]. The laser output is amplified and spectrally broadened to an octave to enable self-referenced detection of the carrier envelope offset frequency, f_{ceo}. The fourth harmonic of f_{rep} is phase-locked to a reference synthesizer at 999.999 544 MHz, and f_{ceo} is electronically divided by 8 and phase-locked to another synthesizer at 20 MHz. Both of these synthesizers are referenced to the same f_{clk} that is the input to the integrated-photonics synthesizer, yielding a comb against which any frequency of the microcomb or tunable laser output can be compared.

The beat-note frequency between the integrated-photonics synthesizer and the erbium-fibre frequency comb is amplified and bandpass-filtered (45 MHz bandwidth), after which a zero-dead-time frequency counter registers the frequency for a fixed gate time. The rectangular binning, or Π-mode, is used during measurement and for the ADEV analysis. The MDEV analysis applies a triangular averaging window to the frequency data for further information on the noise type. With this analysis, a $\tau^{-3/2}$ slope shows the desired white phase noise performance, and deviation from this slope reveals unwanted flicker phase noise contributes to system performance at longer averaging times. Because the degrees of freedom depend on noise type, we take the conservative estimate of flicker phase noise to derive 95% confidence intervals[39]. The tunable laser PLL also contains an in-loop frequency counter, which showed tight phase-locking of the laser to the microcomb at $<10^{-13}/\tau$, limited by the resolution of the counter. All RF synthesizers in the experimental set-up, auxiliary comb and frequency counter are tied to the same hydrogen maser signal, serving as f_{clk}.

Perspectives and future work. A critical element to operation of the optical synthesizer is the pump laser of the DKS microcombs. We show that the same III−V/Si tunable laser from this work can be used to generate low-noise solitons in the Si₃N₄ microresonator; see Extended Data Fig. 2. Further development is required to stabilize solitons in the high-Q SiO₂ microresonator with the III−V/Si tunable laser, although we observe modulation instability (non-soliton) Kerr combs and their transient decay through the Kerr soliton stability regime. Further technical improvement of the III−V/Si tunable laser would probably permit soliton stabilization. At present, we require an optical power of 80 mW for the SiO₂ comb, 160 mW on-chip for the Si₃N₄ comb and 9 mW on-chip for the PPLN device. In each case, we anticipate improving the chip-device performance to be compatible with available integrated-laser power levels to support further integration of our frequency synthesizer. In future implementations of our optical-frequency synthesizer, technical improvements such as improved on and off chip coupling, long wavelength SOAs[40] and higher efficiency second-harmonic generation[41] would make the 1,998-nm diode laser unnecessary.

Data availability. The data sets generated and/or analysed during the current study are available from the corresponding authors on reasonable request.

33. Komljenovic, T. et al. Widely tunable narrow-linewidth monolithically integrated external-cavity semiconductor lasers. *IEEE J. Sel. Top. Quantum Electron.* **21**, 214–222 (2015).
34. Briles, T. C. et al. Kerr-microresonator solitons for accurate carrier-envelope-frequency stabilization. Preprint at https://arxiv.org/abs/1711.06251 (2017).
35. Yang, K. Y. et al. Bridging ultrahigh-Q devices and photonic circuits. *Nat. Photonics* (2018).
36. Stone, J. et al. Thermal and nonlinear dissipative-soliton dynamics in Kerr microresonator frequency combs. Preprint at https://arxiv.org/abs/1708.08405 (2017).
37. Bluestone, A. et al. Heterodyne-based hybrid controller for wide dynamic range optoelectronic frequency synthesis. *Opt. Express* **25**, 29086–29097 (2017).
38. Ycas, G., Osterman, S. & Diddams, S. A. Generation of a 660–2100 nm laser frequency comb based on an erbium fiber laser. *Opt. Lett.* **37**, 2199–2201 (2012).
39. Greenhall, C. A. & Riley, W. J. in *Proc. PTTI 2003*, 267–280 (2003).
40. Volet, N. et al. Semiconductor optical amplifiers at 2.0-μm wavelength on silicon. *Laser Photonics Rev.* **11**, 1600165 (2017).
41. Chang, L. et al. Thin film wavelength converters for photonic integrated circuits. *Optica* **3**, 531–535 (2016).
42. Srinivasan, S. et al. Coupled-ring-resonator-mirror-based heterogeneous III–V silicon tunable laser. *IEEE Photonics J.* **7**, 2700908 (2015).
43. Del'Haye, P., Papp, S. B. & Diddams, S. A. Hybrid electro-optically modulated microcombs. *Phys. Rev. Lett.* **109**, 263901 (2012).
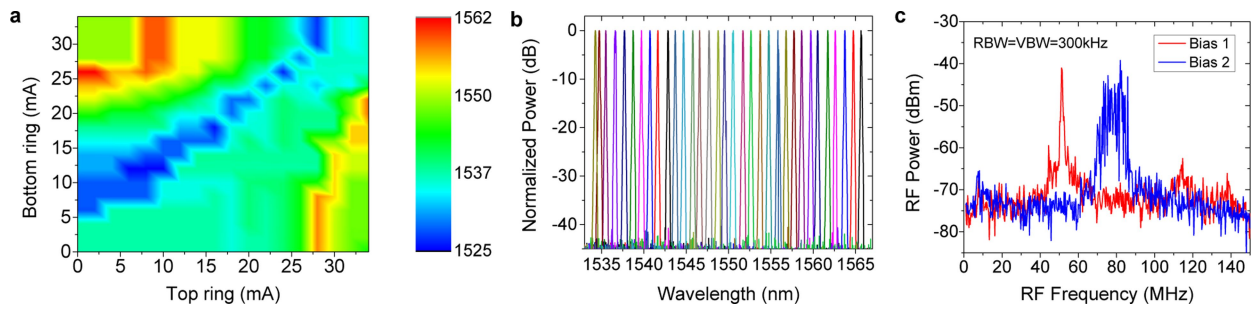
Extended Data Fig. 1 | Tuning details for III−V/Si laser. a, Typical tuning map of the III−V/Si tunable laser's peak wavelength in nanometres versus current applied to each heater above the ring resonators. **b**, Normalized optical spectra showing >40 dB of side-mode suppression ratio across the tuning range. **c**, Typical unlocked RF beat notes between the tunable laser and the auxiliary comb for two different biases of the phase section.

Careful control of the heater is required to reach all wavelengths in the tuning range, and reduction of the laser linewidth (blue to red) through longitudinal mode alignment and the optical feedback effect[42] is required to achieve the best phase-locking performance to the microcombs. RBW, resolution bandwidth, VBW, video bandwidth.
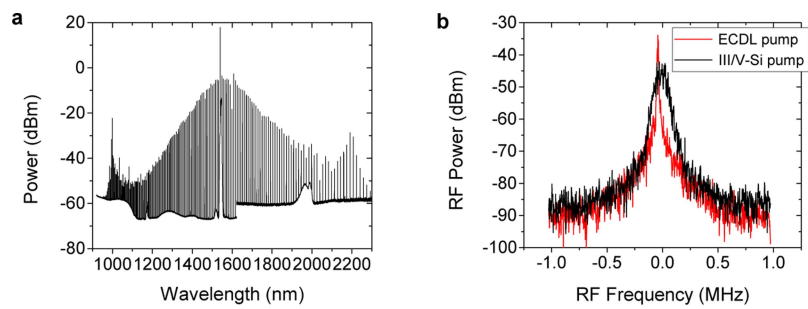
Extended Data Fig. 2 | Demonstration of pumping the Si₃N₄ THz microcomb with the III−V/Si laser. a, Output optical spectrum of the THz microcomb showing dual-dispersive waves, as measured on two optical spectrum analysers. **b**, Comparison of electro-optic repetition rate detection[43] when using the same III−V/Si laser (black) and external cavity diode laser (ECDL, red) from the main experiment to pump the THz microcomb.